

Achieving high-resolution photoelectron spectroscopy from a broadband femtosecond laser pulse

Shian Zhang,* Chenhui Lu, Tianqing Jia, and Zhenrong Sun†

State Key Laboratory of Precision Spectroscopy and Department of Physics, East China Normal University, Shanghai 200062, People's Republic of China

(Received 3 April 2012; published 23 July 2012)

Femtosecond-induced resonance-enhanced multiphoton-ionization photoelectron spectroscopy (REMPI-PS) suffers from poor spectral resolution due to the large laser spectral bandwidth. In this paper, we present a scheme to achieve high-resolution REMPI-PS in the potassium atom by shaping the ultrashort femtosecond laser pulse. Our results show that the REMPI-PS bandwidth can be narrowed by several tens of times with a cubic spectral phase modulation, and thus high-resolution REMPI-PS and the fine structure of the energy-level diagram for multiple excited states can be obtained in spite of the broadband femtosecond laser pulse. Furthermore, we explain the physical control mechanism of the narrowband REMPI-PS by considering the two-photon power spectrum.

DOI: 10.1103/PhysRevA.86.012513

PACS number(s): 33.60.+q, 32.80.Qk, 32.80.Rm

With the advent of the ultrafast pulse-shaping technique, by modulating the laser spectral phase or/and amplitude in the frequency domain using a pulse shaper, such a shaped laser pulse with an almost arbitrary temporal distribution can be obtained [1], and this opens a new opportunity to control various nonlinear optical processes [2–5]. According to the actual requirements, coherent control by the pulse-shaping technique can be performed by an open-loop scheme with a predesigned spectral phase or/and amplitude pattern or a closed-loop scheme based on a learning algorithm [1]. Nowadays, the quantum control strategy making use of a shaped femtosecond laser pulse has been successfully applied in the control of two- and multiphoton absorption [6–9], high-order-harmonic generation [10], stimulated Raman scattering [11,12], coherent anti-Stokes Raman scattering spectroscopy [13–17], photoionization and photodissociation [18–21], and so on.

Resonance-enhanced multiphoton-ionization photoelectron spectroscopy (REMPI-PS) has attracted considerable attention in the past two decades due to its potential applications in characterizing the structure of excited states and studying the dynamical processes of photoionization and photodissociation [22–29]. A femtosecond laser pulse has proven to be a well-established tool in inducing REMPI-PS, but an inevitable problem for the technique is poor spectral resolution due to the large laser spectral bandwidth. Therefore, how to narrow the femtosecond-induced REMPI-PS bandwidth and obtain high-resolution REMPI-PS is an interesting research question. In this paper, we theoretically show that narrowband REMPI-PS in the potassium (K) atom can be obtained by shaping the ultrashort femtosecond laser pulse with a cubic spectral phase modulation. This narrowband REMPI-PS is several tens of times narrower than the PS from a transform-limited laser pulse, and thus high-resolution REMPI-PS and the fine structure of the energy-level diagram for multiple excited states can be obtained with this simple modulation. Moreover, we also show that the modulation of the narrowband REMPI-PS can be explained by the two-photon power spectrum.

Figure 1 shows the excitation scheme of the resonance-enhanced multiphoton-ionization process in the K atom induced by an ultrashort femtosecond laser pulse $E(t)$. Here, the transition from the ground state $4S_{1/2}$ to the excited state $4P_{1/2}$ or $4P_{3/2}$ is caused by one-photon absorption, and finally the populations in the excited states $4P_{1/2}$ and $4P_{3/2}$ are ionized by two-photon absorption. Thus, the $(1+2)$ REMPI-PS $P(E_v)$ can be approximated as [18,30–33]

$$P(E_v) \propto \int_{-\infty}^{+\infty} E^2(t) C_{4P_{1(3)/2}}(t) \times \exp[i(E_v + E_I - E_{4P_{1(3)/2}})t/\hbar] dt, \quad (1)$$

where E_I is the ionization energy from the ground state $4S_{1/2}$ and $E_{4P_{1(3)/2}}$ is the eigenenergy of the excited state $4P_{1/2}$ or $4P_{3/2}$. $C_{4P_{1(3)/2}}(t)$ describes the time-dependent probability amplitude in the excited state $4P_{1/2}$ or $4P_{3/2}$, which is obtained by numerically solving the time-dependent Schrödinger equation, and written as

$$i\hbar \frac{\partial}{\partial t} \begin{pmatrix} C_{4S_{1/2}} \\ C_{4P_{1/2}} \\ C_{4P_{3/2}} \end{pmatrix} = \begin{bmatrix} 0 & \Omega_{4S_{1/2} \rightarrow 4P_{1/2}}(t) & \Omega_{4S_{1/2} \rightarrow 4P_{3/2}}(t) \\ \Omega_{4S_{1/2} \rightarrow 4P_{1/2}}^*(t) & E_{4P_{1/2}} & 0 \\ \Omega_{4S_{1/2} \rightarrow 4P_{3/2}}^*(t) & 0 & E_{4P_{3/2}} \end{bmatrix} \times \begin{pmatrix} C_{4S_{1/2}} \\ C_{4P_{1/2}} \\ C_{4P_{3/2}} \end{pmatrix}, \quad (2)$$

where $\Omega_{4S_{1/2} \rightarrow 4P_{1(3)/2}}(t)$ is the laser Rabi frequency with $\Omega_{4S_{1/2} \rightarrow 4P_{1(3)/2}}(t) = \mu_{4S_{1/2} \rightarrow 4P_{1(3)/2}} E(t)/\hbar$, and $\mu_{4S_{1/2} \rightarrow 4P_{1(3)/2}}$ is the transition dipole moment from the ground state $4S_{1/2}$ to the excited state $4P_{1/2}$ or $4P_{3/2}$.

Here, we utilize a cubic spectral phase modulation $\Phi(\omega) = \alpha(\omega - \delta\omega)^3$ to control the REMPI-PS, where α and $\delta\omega$ are the modulation amplitude and the phase step position, respectively. Figure 2 presents the cubic spectral phase modulation (left panel) and the corresponding temporal intensity profile (right panel) for various α and $\delta\omega$. It can be seen that the shaped laser pulse is asymmetric with an intense

*sazhang@phy.ecnu.edu.cn

†zrsun@phy.ecnu.edu.cn

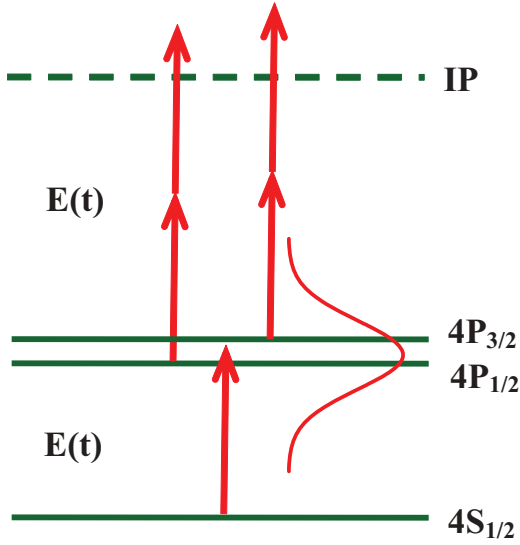


FIG. 1. (Color online) The excitation scheme of the (1+2) resonance-enhanced multiphoton-ionization process in a potassium atom induced by an ultrashort femtosecond laser pulse $E(t)$. The transition from the ground state $4S_{1/2}$ to the excited state $4P_{1/2}$ or $4P_{3/2}$ is caused by one-photon absorption, and the populations in the excited states $4P_{1/2}$ and $4P_{3/2}$ are ionized by two-photon absorption.

initial pulse followed or preceded by a pulse sequence with decaying amplitude. The magnitude of α (i.e., $|\alpha|$) controls the number of pulses; the number increases with increase of $|\alpha|$ [see Figs. 2(a) and 2(b)]. The sign of α (i.e., $\pm\alpha$) decides the time direction of the shaped pulse; $+\alpha$ leads to a series of postpulses whereas $-\alpha$ causes a series of prepulses [see Figs. 2(b) and 2(d)]. $\delta\omega$ controls the separation of the pulse sequence; the separation decreases with increase of

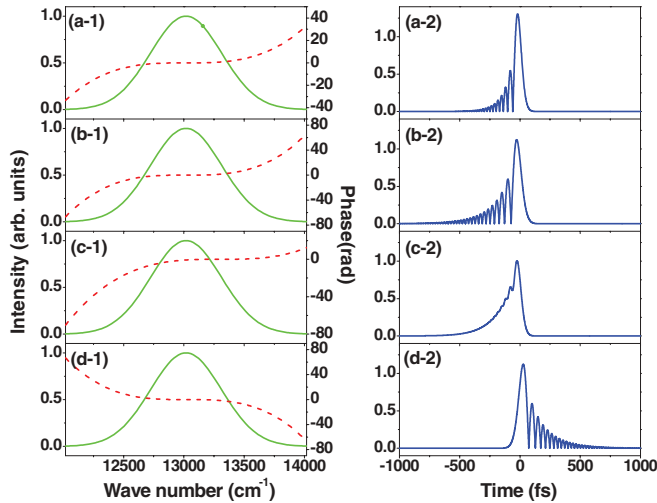


FIG. 2. (Color online) The spectral phase modulation with the cubic function $\Phi(\omega) = \alpha(\omega - \delta\omega)^3$ (left panel) and the corresponding temporal intensity profile (right panel) for the modulation amplitudes and phase step positions $\alpha = 5 \times 10^3 \text{ fs}^3$ and $\delta\omega = 13018 \text{ cm}^{-1}$ (a), $\alpha = 1 \times 10^4 \text{ fs}^3$ and $\delta\omega = 13018 \text{ cm}^{-1}$ (b), $\alpha = 5 \times 10^3 \text{ fs}^3$ and $\delta\omega = 13300 \text{ cm}^{-1}$ (c), and $\alpha = -1 \times 10^4 \text{ fs}^3$ and $\delta\omega = 13018 \text{ cm}^{-1}$ (d).

the magnitude of $\delta\omega - \omega_L$ (i.e., $|\delta\omega - \omega_L|$) [see Figs. 2(a) and 2(c)], where ω_L is the laser's central frequency.

In our simulation, the transition frequencies from the ground state $4S_{1/2}$ to the excited states $4P_{1/2}$ and $4P_{3/2}$ in the K atom are, respectively, $\omega_{4S_{1/2} \rightarrow 4P_{1/2}} = 12989 \text{ cm}^{-1}$ and $\omega_{4S_{1/2} \rightarrow 4P_{3/2}} = 13047 \text{ cm}^{-1}$, and their separation is 58 cm^{-1} . The ionization energy from the ground state $4S_{1/2}$ is $E_I = 4.34 \text{ eV}$, corresponding to a frequency of 35004 cm^{-1} . The laser central frequency is set to be $\omega_L = 13018 \text{ cm}^{-1}$, which is in the middle of the two transition frequencies $\omega_{4S_{1/2} \rightarrow 4P_{1/2}}$ and $\omega_{4S_{1/2} \rightarrow 4P_{3/2}}$, the laser pulse duration [full width at half maximum (FWHM)] is $\tau = 30 \text{ fs}$, and the laser intensity is $I = 1 \times 10^{10} \text{ W/cm}^2$. In our calculation, the shaped laser pulse in the frequency domain is given by $E_s(\omega) = E(\omega) \times \exp[i \times \Phi(\omega)]$, where $E(\omega)$ is the Fourier transform of the unshaped laser pulse $E(t)$, and the shaped laser pulse in the time domain $E_s(t)$ is given by the inverse Fourier transform of $E_s(\omega)$. By substituting $E_s(t)$ into Eqs. (1) and (2), the photoelectron spectrum $P(E_v)$ induced by the shaped laser pulse can be obtained.

First, we consider the case of the resonance-enhanced multiphoton-ionization process only through the excited state $4P_{1/2}$. Figure 3 shows the photoelectron spectra through the excited state $4P_{1/2}$ induced by the shaped laser pulse with the phase step position $\delta\omega = 13018 \text{ cm}^{-1}$ for the modulation amplitudes $\alpha = 2 \times 10^3$ (red solid line), 2×10^4 (green dashed line), and $2 \times 10^5 \text{ fs}^3$ (blue dotted line) [Fig. 3(a)], and $\alpha = -2 \times 10^3$ (red solid line), -2×10^4 (green dashed line), and $-2 \times 10^5 \text{ fs}^3$ (blue dotted line) [Fig. 3(b)]. One can see that the photoelectron spectrum is narrowed when $|\alpha|$ increases. The bandwidth (FWHM) of the photoelectron spectrum is about 0.138 eV for the transform-limited laser pulse, while it is only about 0.003 eV for the shaped laser pulse with $\alpha = -2 \times 10^5 \text{ fs}^3$, i.e., it is narrowed by several tens of times. By comparing the photoelectron spectra for $+\alpha$ and $-\alpha$, it can be seen that the photoelectron intensity is increased for $-\alpha$ while it is decreased for $+\alpha$, and the photoelectron spectrum

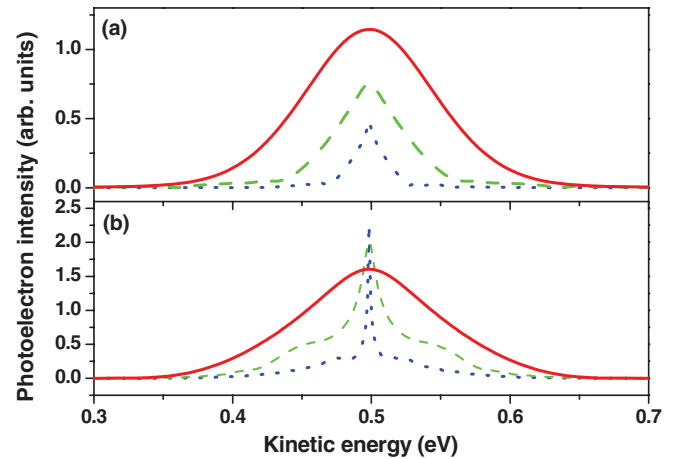


FIG. 3. (Color online) The photoelectron spectra through the excited state $4P_{1/2}$ induced by a shaped laser pulse with phase step position $\delta\omega = 13018 \text{ cm}^{-1}$ for the modulation amplitudes $\alpha = 2 \times 10^3$ (red solid line), 2×10^4 (green dashed line), and $2 \times 10^5 \text{ fs}^3$ (blue dotted line) (a), and $\alpha = -2 \times 10^3$ (red solid line), -2×10^4 (green dashed line), and $-2 \times 10^5 \text{ fs}^3$ (blue dotted line) (b).

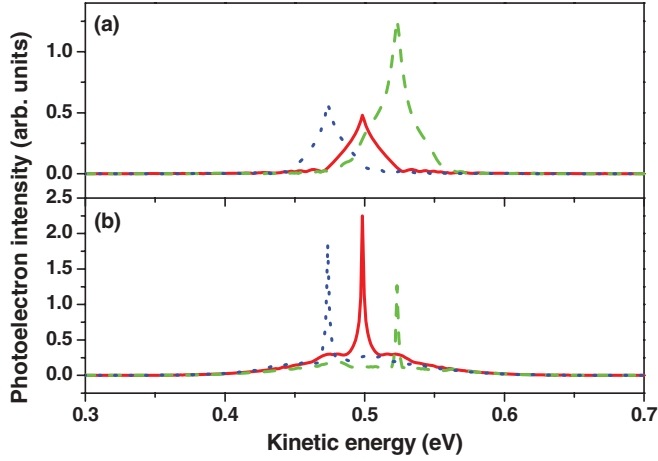


FIG. 4. (Color online) The photoelectron spectra through the excited state $4P_{1/2}$ induced by a shaped laser pulse with phase step positions $\delta\omega = 12918$ (blue dotted lines), 13018 (red solid lines), and 13118 cm^{-1} (green dashed lines) for the modulation amplitudes $\alpha = 2 \times 10^5$ (a) and -2×10^5 fs^3 (b).

for $-\alpha$ is much narrower than that for $+\alpha$ with the same value of $|\alpha|$, which illustrates that $-\alpha$ has more advantage than $+\alpha$ in achieving narrowband photoelectron spectroscopy.

Figure 4 shows the photoelectron spectra through the excited state $4P_{1/2}$ induced by the shaped laser pulse with the phase step positions $\delta\omega = 12918$ (blue dotted lines), 13018 (red solid lines), and 13118 cm^{-1} (green dashed lines) for the modulation amplitudes $\alpha = 2 \times 10^5$ [Fig. 4(a)] and -2×10^5 fs^3 [Fig. 4(b)]. The maximal photoelectron intensities for the phase step positions $\delta\omega = 12918$, 13018 , and 13118 cm^{-1} are obtained at the kinetic energies of 0.4736 , 0.4984 , and 0.5232 eV, respectively. It can be seen that the maximal photoelectron intensities for different phase step positions occur at different kinetic energies, while the energy difference between twice the photon energy at the phase step position (i.e., $2E_p^{\delta\omega}$) and the kinetic energy corresponding to the maximal photoelectron intensity (i.e., E_v^{\max}) is constant, and is equal to the ionization energy from the excited state $4P_{1/2}$ (i.e., E_Δ), where $E_\Delta = E_I - E_{4P_{1/2}}$. That is to say, the four parameters, the photon energy at the phase step position $E_p^{\delta\omega}$, the kinetic energy corresponding to the maximal photoelectron intensity E_v^{\max} , the ionization energy E_I , and the eigenenergy of the excited state $4P_{1/2}$ $E_{4P_{1/2}}$, satisfy the relation $E_I + E_v^{\max} = E_{4P_{1/2}} + 2E_p^{\delta\omega}$. Thus, we can further deduce that the maximal photoelectron intensity for the shaped laser pulse is obtained at the kinetic energy of $E_{4P_{1/2}} + 2E_p^{\delta\omega} - E_I$.

Based on the relation $E_I + E_v^{\max} = E_{4P_{1/2}} + 2E_p^{\delta\omega}$, $E_{4P_{1/2}}$ can be calculated if E_v^{\max} and $E_p^{\delta\omega}$ are known, and thus the excited state $4P_{1/2}$ can be labeled, which will provide a feasible scheme to study the excited-state structure. There are two ways to achieve E_v^{\max} and $E_p^{\delta\omega}$. One is to measure the photoelectron spectrum as shown in Fig. 4, and the other is to measure the photoelectron intensity at a given kinetic energy by scanning the phase step position $\delta\omega$. Figure 5 presents the photoelectron intensity at the kinetic energy of 0.4984 eV through the excited state $4P_{1/2}$ as a function of the phase step position $\delta\omega$ for the modulation amplitudes $\alpha = 2 \times 10^5$ [Fig. 5(a)] and -2×10^5 fs^3 [Fig. 5(b)]. The photoelectron intensity is

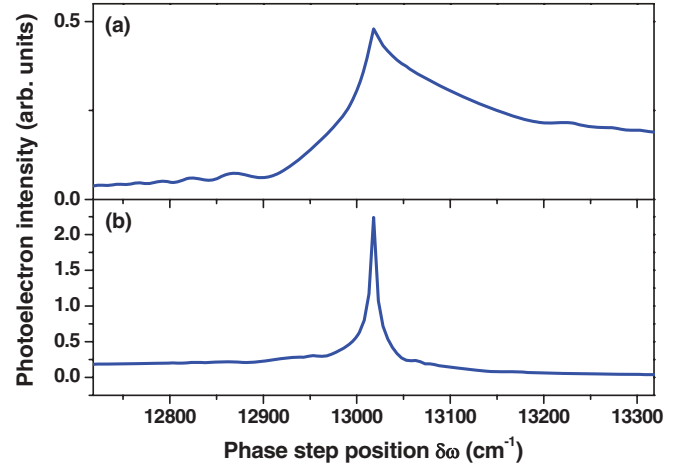


FIG. 5. (Color online) The photoelectron intensity at the kinetic energy of 0.4984 eV through the excited state $4P_{1/2}$ as a function of phase step position $\delta\omega$ for the modulation amplitudes $\alpha = 2 \times 10^5$ (a) and -2×10^5 fs^3 (b).

maximum at the phase step position $\delta\omega = 13018$ cm^{-1} , which is consistent with the results in Fig. 4.

Since narrowband REMPI-PS can be obtained by shaping an ultrashort femtosecond laser pulse with a cubic spectral phase modulation and the maximal photoelectron intensity occurs at the kinetic energy of $E_{4P_{1/2}} + 2E_p^{\delta\omega} - E_I$, high-resolution REMPI-PS through the two excited states $4P_{1/2}$ and $4P_{3/2}$ can be achieved. Figure 6 shows the photoelectron spectra through both the excited states $4P_{1/2}$ and $4P_{3/2}$ (green solid lines) induced by the transform-limited laser pulse [Fig. 6(a)] and the shaped laser pulse with the phase step position $\delta\omega = 13018$ cm^{-1} for the modulation amplitudes $\alpha = 2 \times 10^5$ [Fig. 6(b)] and -2×10^5 fs^3 [Fig. 6(c)], together with the photoelectron spectra for only the excited state $4P_{1/2}$ (red dashed lines) or $4P_{3/2}$ (blue dotted lines). Only a single

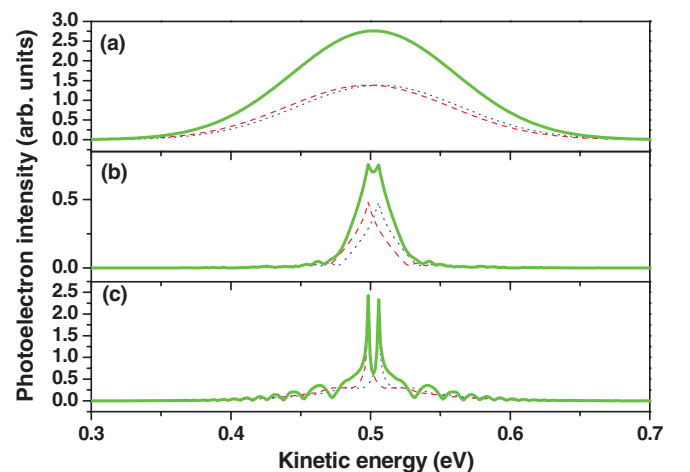


FIG. 6. (Color online) The photoelectron spectra through both the excited states $4P_{1/2}$ and $4P_{3/2}$ (green solid lines) induced by the transform-limited laser pulse (a) and the shaped laser pulse with phase step position $\delta\omega = 13018$ cm^{-1} for the modulation amplitudes $\alpha = 2 \times 10^5$ (b) and -2×10^5 fs^3 (c), together with the photoelectron spectra for only the excited state $4P_{1/2}$ (red dashed lines) or $4P_{3/2}$ (blue dotted lines).

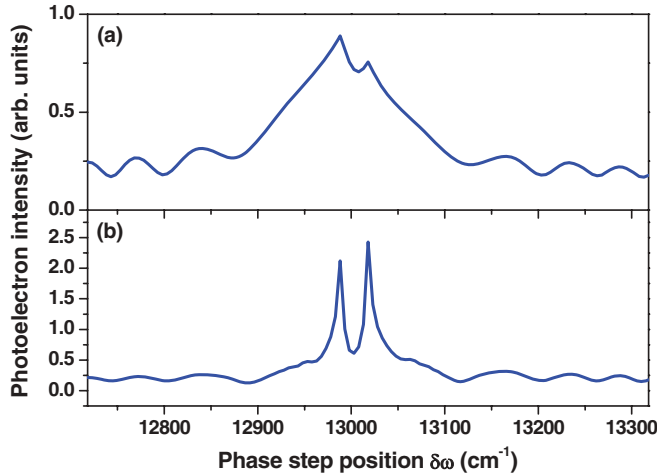


FIG. 7. (Color online) The photoelectron intensity at the kinetic energy of 0.4984 eV through both the excited states $4P_{1/2}$ and $4P_{3/2}$ as a function of the phase step position $\delta\omega$ for the modulation amplitudes $\alpha = 2 \times 10^5$ (a) and -2×10^5 fs³ (b).

broadband peak is observed for the transform-limited laser pulse [see Fig. 6(a)], while two distinct peaks at the kinetic energies of 0.4984 and 0.5058 eV are observed for the shaped laser pulse [see Figs. 6(b) and 6(c)], which are related to the two excited states $4P_{1/2}$ and $4P_{3/2}$.

Similarly, the fine structure of the energy-level diagram for the two excited states $4P_{1/2}$ and $4P_{3/2}$ can also be labeled by measuring the photoelectron intensity at a given kinetic energy and scanning the phase step position $\delta\omega$. Figure 7 shows the photoelectron intensity at the kinetic energy of 0.4984 eV through both the two excited states $4P_{1/2}$ and $4P_{3/2}$ as a function of the phase step position $\delta\omega$ for the modulation amplitudes $\alpha = 2 \times 10^5$ [Fig. 7(a)] and -2×10^5 fs³ [Fig. 7(b)]. Two distinct peaks at phase step positions $\delta\omega = 12989$ and 13018 cm⁻¹ are observed. According to the relation $E_I + E_v^{\max} = E_{4P_{1(3)/2}} + 2E_P^{\delta\omega}$, $E_{4P_{1/2}}$ and $E_{4P_{3/2}}$ are respectively calculated as 1.6104 and 1.6176 eV, corresponding to the frequencies of 12989 and 13047 cm⁻¹, which are consistent with the transition frequencies of the two excited states $4P_{1/2}$ and $4P_{3/2}$, $\omega_{4S_{1/2} \rightarrow 4P_{1/2}}$ and $\omega_{4S_{1/2} \rightarrow 4P_{3/2}}$, mentioned above.

A previous study showed that coherent control of the two-photon absorption by a shaped laser pulse can be explained by considering the power spectrum of $E^2(t)$ (i.e., the two-photon power spectrum) [34]. Here, we also employ the two-photon power spectrum to explain the physical control mechanism of the narrowband REMPI-PS since the populations in the excited states $4P_{1/2}$ and $4P_{3/2}$ are ionized by two-photon absorption. Figure 8 presents the two-photon power spectrum of the shaped laser pulse for the modulation amplitudes and phase step positions $\alpha = -2 \times 10^4$ fs³ and $\delta\omega = 13018$ cm⁻¹ [Fig. 8(a)], $\alpha = -2 \times 10^5$ fs³ and $\delta\omega = 13018$ cm⁻¹ [Fig. 8(b)],

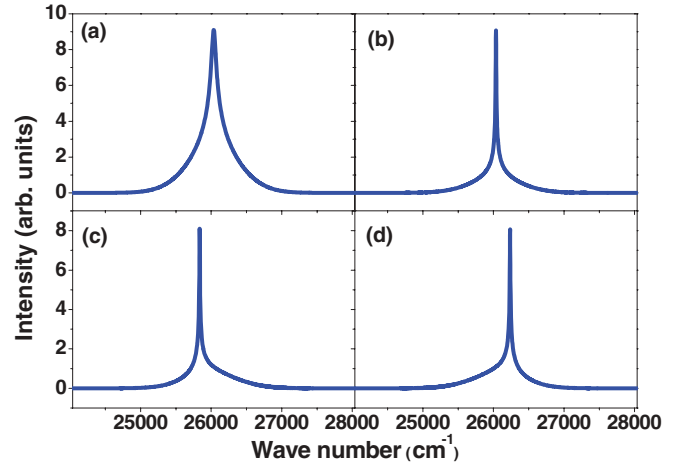


FIG. 8. (Color online) The two-photon power spectra of the shaped laser pulse for the modulation amplitudes and phase step positions $\alpha = -2 \times 10^4$ fs³ and $\delta\omega = 13018$ cm⁻¹ (a), $\alpha = -2 \times 10^5$ fs³ and $\delta\omega = 13018$ cm⁻¹ (b), $\alpha = -2 \times 10^5$ fs³ and $\delta\omega = 12918$ cm⁻¹ (c), and $\alpha = -2 \times 10^5$ fs³ and $\delta\omega = 13118$ cm⁻¹ (d).

$\alpha = -2 \times 10^5$ fs³ and $\delta\omega = 12918$ cm⁻¹ [Fig. 8(c)], and $\alpha = -2 \times 10^5$ fs³ and $\delta\omega = 13118$ cm⁻¹ [Fig. 8(d)]. As can be seen, increasing the modulation amplitude $|\alpha|$ will reduce the bandwidth of the power spectrum [see Figs. 8(a) and 8(b)], and varying the phase step position $\delta\omega$ will change the position of the power spectrum [see Figs. 8(c) and 8(d)]. Obviously, the modulation of the two-photon power spectrum is the same as for the REMPI-PS (see Figs. 3 and 4). Furthermore, we theoretically find that a laser pulse shaped by the spectral phase modulation $\Phi(\omega) = \alpha(\omega - \delta\omega)^{2m+1}$ ($m = 1, 2, 3, \dots$) can have a narrower two-photon power spectrum. In other words, the REMPI-PS can be narrowed by the $(2m + 1)$ th power of the spectral phase modulation.

In conclusion, we have theoretically shown that, by shaping an ultrashort femtosecond laser pulse with a cubic spectral phase modulation, the bandwidth of the $(1+2)$ REMPI-PS in a K atom can be reduced by several tens of times, and thus high-resolution REMPI-PS and the fine structure of the energy-level diagram for multiple excited states can be obtained. Furthermore, we used the two-photon power spectrum to explain the physical control mechanism of the narrowband REMPI-PS. We believe that these theoretical results have promising applications in studying atomic and molecular structures, and we expect them to be extended to the control of the photoelectron spectroscopy in various resonance-enhanced multiphoton-ionization processes.

This work was partly supported by Ministry of Education of China (Grant No. 30800), the National Natural Science Fund (Grants No. 11004060, No. 11027403, and No. 51132004), and the Shanghai Municipal Science and Technology Commission (Grants No. 10XD1401800 and No. 10JC1404500).

[1] A. M. Weiner, *Rev. Sci. Instrum.* **71**, 1929 (2000).
 [2] C. Brif, R. Chakrabarti, and H. Rabitz, *New J. Phys.* **12**, 075008 (2010).

[3] Y. Silberberg, *Annu. Rev. Phys. Chem.* **60**, 277 (2009).
 [4] P. Nuernberger, G. Nogat, T. Brixner, and G. Gerber, *Phys. Chem. Chem. Phys.* **9**, 2470 (2007).

- [5] D. Goswami, *Phys. Rep.* **374**, 385 (2003).
- [6] S. Zhang, H. Zhang, T. Jia, Z. Wang, and Z. Sun, *Phys. Rev. A* **80**, 043402 (2009).
- [7] B. D. Bruner, H. Suchowski, N. V. Vitanov, and Y. Silberberg, *Phys. Rev. A* **81**, 063410 (2010).
- [8] V. V. Lozovoy, L. Pastirk, K. A. Walowicz, and M. Dantus, *J. Chem. Phys.* **118**, 3187 (2003).
- [9] Z. Amitay, A. Gandman, L. Chuntanov, and L. Rybak, *Phys. Rev. Lett.* **100**, 193002 (2008).
- [10] R. Bartels, S. Backus, E. Zeek, L. Misoguti, G. Vdovin, I. P. Chris-tov, M. M. Murnane, and H. C. Kapteyn, *Nature (London)* **406**, 164 (2000).
- [11] S. A. Malinovskaya, P. H. Bucksbaum, and P. R. Berman, *Phys. Rev. A* **69**, 013801 (2004).
- [12] S. A. Malinovskaya, *Opt. Lett.* **33**, 2245 (2008).
- [13] A. C. W. van Rhijn, M. Jurna, A. Jafarpour, J. L. Herek, and H. L. Offerhaus, *J. Raman Spectrosc.* **42**, 1859 (2011).
- [14] S. Zhang, H. Zhang, T. Jia, Z. Wang, and Z. Sun, *J. Chem. Phys.* **132**, 044505 (2010).
- [15] O. Katz, J. M. Levitt, E. Grinvald, and Y. Silberberg, *Opt. Express* **18**, 22693 (2010).
- [16] V. Patel, V. S. Malinovsky, and S. Malinovskaya, *Phys. Rev. A* **81**, 063404 (2010).
- [17] J. Konradi, A. K. Singh, and A. Materny, *J. Photochem. Photobiol., A* **180**, 289 (2006).
- [18] M. Wollenhaupt, T. Bayer, N. V. Vitanov, and T. Baumert, *Phys. Rev. A* **81**, 053422 (2010).
- [19] M. Krug, T. Bayer, M. Wollenhaupt, C. Sarpe-Tudoran, T. Baumert, S. S. Ivanov, and N. V. Vitanov, *New J. Phys.* **11**, 105051 (2009).
- [20] V. S. Prabhudesai, U. Lev, A. Natan, B. D. Bruner, A. Diner, O. Heber, D. Strasser, D. Schwalm, I. Ben-Itzhak, J. J. Hua, B. D. Esry, Y. Silberberg, and D. Zajfman, *Phys. Rev. A* **81**, 023401 (2010).
- [21] J. Plenge, A. Wirsing, I. Wagner-Drebenstedt, I. Halfpap, B. Kieling, B. Wassermann, and E. Rühl, *Phys. Chem. Chem. Phys.* **13**, 8705 (2011).
- [22] J. Zhang, C. Harthcock, and W. Kong, *J. Phys. Chem. A* **116**, 1551 (2012).
- [23] J. Zhang, C. Harthcock, F. Y. Han, and W. Kong, *J. Chem. Phys.* **135**, 244306 (2011).
- [24] L. Shen, B. L. Zhang, and A. G. Suits, *J. Phys. Chem. A* **114**, 3114 (2010).
- [25] V. Blanchet, S. Boye, S. Zamith, A. Campos, B. Girard, J. Lievin, and D. Gauyacq, *J. Chem. Phys.* **119**, 3751 (2003).
- [26] J. Liu, H.-T. Kim, and S. L. Anderson, *J. Chem. Phys.* **114**, 9797 (2001).
- [27] N. P. Morre and R. J. Levis, *J. Chem. Phys.* **112**, 1316 (2000).
- [28] C. R. Scherper, J. Kuijt, W. J. Buma, and C. A. de Lange, *J. Chem. Phys.* **109**, 7844 (1998).
- [29] M. R. Dobber, W. J. Buma, and C. A. de Lange, *J. Chem. Phys.* **99**, 836 (1993).
- [30] M. Wollenhaupt, A. Präkelt, C. Sarpe-Tudoran, D. Liese, T. Bayer, and T. Baumert, *Phys. Rev. A* **73**, 063409 (2006).
- [31] M. Wollenhaupt, A. Präkelt, C. Sarpe-Tudoran, D. Liese, and T. Baumert, *Appl. Phys. B* **82**, 183 (2006).
- [32] M. Wollenhaupt, A. Präkelt, C. Sarpe-Tudoran, D. Liese, and T. Baumert, *J. Phys. B* **7**, S270 (2005).
- [33] M. Wollenhaupt, V. Engle, and T. Baumert, *Annu. Rev. Phys. Chem.* **56**, 25 (2005).
- [34] P. H. Bucksbaum, *Nature (London)* **396**, 217 (1998).